Power Generation by Artificial Typhoon

Ichizo Aoki

Introduction

The purpose of this study is to propose alternative energy sources substituting conventional fossil fuels and nuclear fission and or fusion. Those conventional energy sources are all earth-derived and have limited supply. Peak of oil production is expected to arrive soon as estimated by logistic model shown in Fig.-1. Peak time may arrive around year of 2020 when ultimate recoverable oil reserve is 3 trillion of barrels as estimated by US Geological Survey. If ultimate recoverable oil reserve is 1.8 trillion of barrels as estimated by Colin Campbell, peak time is around year of 2005.

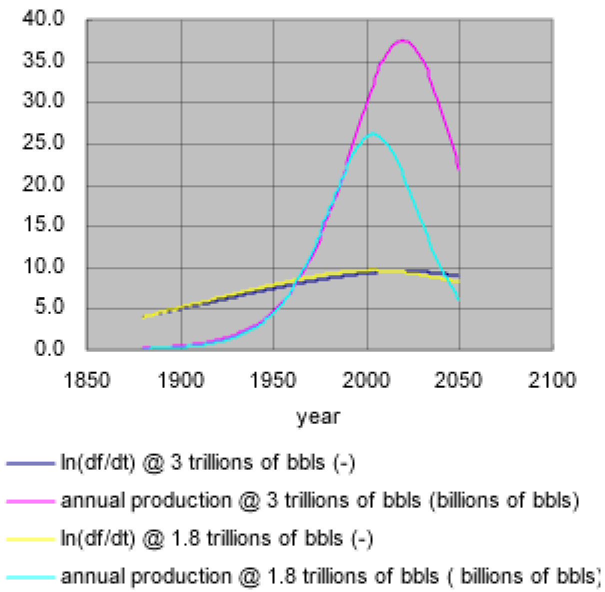

Fig.-1 Peak of Oil Production by Logistic Model

On the other hand, solar energy surpasses the earth-derived energy in quantities, but given in dispersed form. The most promising technology would be solar cells in its high conversion of more than 10 % of solar emission into electricity. But it's high cost is prohibiting to become major source. Conversion efficiency of bio-mass is below 1% and ecologically prohibiting large development in the future even if it is sustainable.

Windfirm and hydraulic power using natural wind and rain are already developed extensively in many countries, as the cost is competitive to the conventional energy. But wind firm and hydraulic power are very site specific.

In 1982 to 1989. The German Ministry of Research and Technology conducted a prototype test in Manzanare, Spain. A German company called Schlaich Bergermann and Partners designed the facility. The circular solar collector having diameter of 237 m warmed up air about 35 °C. Warmed up air is sucked into the bottom of draft duct having the height of 200 m and diameter of 10 m and driven wind turbine placed at the bottom of the duct. The wind turbine generated 60 kW. The solar collector is covered with thin plastic film made of vinyl-fluoride resin and supported by wires and poles. The bare surface of the desert absorbs solar heat and warm up the air bowing above. The plant was successfully operate over 4 years and it was found out that accumulated heat in the earth continued generating wind after sunset.

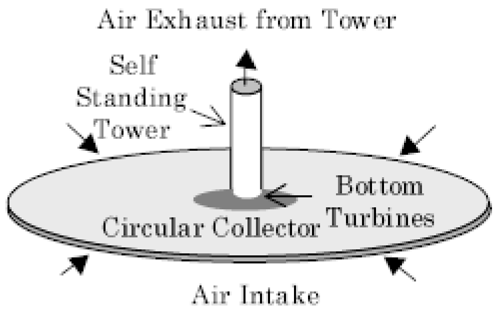

Fig.-2 Australian Project

At the end of 2001, an Australian startup company called EnviroMission announced an ambitious plan to install world's tallest draft tower having the height of 1,000 m and having the diameter of 150 m in the desert of Wentworth

Shire, NSW as illustrated in the Fig.-2. This system can generate power of 200 MW by 32 wind turbines installed at the bottom of the draft tower. The diameter of the circular solar collector for warming air is 5 km. The solar collector is covered with glass and/or thin plastic film and warm up air about 35-40 °C. It was reported that the world first commercial plant cost about Australian \$ of 700 million.

A German company called Schlaich Bergermann and Partners designed the facility.

They called it “Solar Tower”, but it could also be called, as “Power Generation by Artificial Typhoon” as the mechanism of generating wind is similar to typhoon or hurricane.

When the plant operates 333 days in a year and the sun shines 12 hrs/day above your head and more than 80 % of the days are fine days, annual generated power reaches 323 TWh. When needed annual cash flow is 10.67 % of initial investment, and the plant is operated with 5 operators, the unit cost of power generation becomes 20.8 yen/kWh (18.9 cents/kWh).

Needed annual cash flow of 10.67 % of initial investment is based on the conditions summarized in Table-1.

Table-1 Basis of Needed Annual Cash Flow

Items	Figures
Project Life	30 years
Equity	20 % of Initial Investment
Discount Rate	8%
Income Tax Rate	40%
Depreciation Period	17years, with flat rate
Interest Rate	4 %
Debt Service Period	14 years
Property Tax	1.4 % of Initial Investment
Insurance Premium	5% of Initial Investment
Maintenance Cost	0.1 % of Initial Investment
Administration Cost	1 % of Initial Investment

It is also assumed that replacement cost of the aged cover is 20% of initial investment and debt repayment is done by equal annual installment.

Discounted cash flow is illustrated in Fig.-3. It was assumed that labor rate is 6 million yen/year.

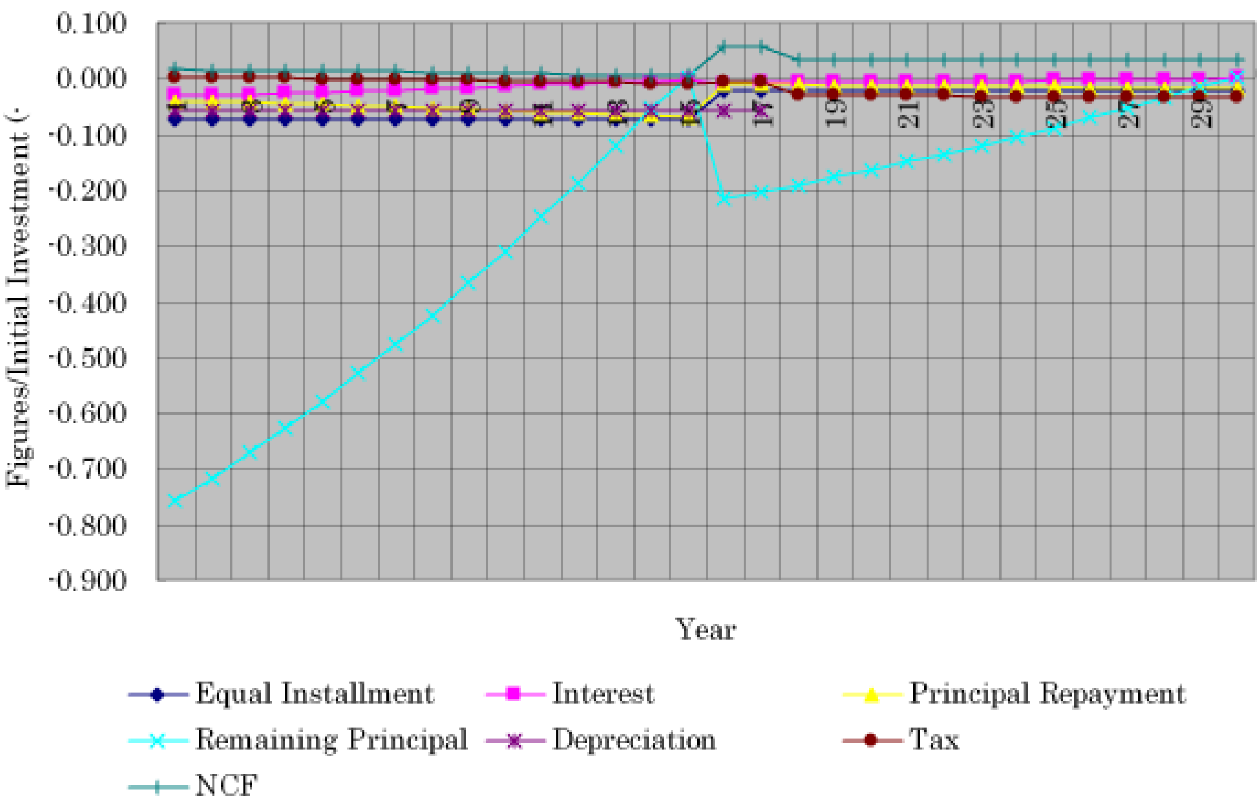

Fig.-3 Discounted Cash Flow

The unit cost of power generation of 20.8 yen/kWh is a bit high compared to the conventional power plant like 5.9 yen/kWh of coal fired, but seemed promising. All other conventional power cost falls in the same range like 10.9 yen/kWh of oil fired, 6.3 yen/kWh of LNG fired, 5.6 yen/kWh of nuclear, 11 yen/kWh of hydraulic and 9.4 to 13.1 yen/kWh of windfirm. But unit cost of 20.7 yen/kWh is far lower than 74 yen/kWh of solar cells.

I had made an engineering model for reverse engineering of the test plant in Manzanare and commercial plant of Australian project and found my model has a good agreement with the published data.

In the course of the study, I found a more elegant way of recovering more power from the system by installing the wind turbines at the top of the draft duct rather than installing the wind turbines at the bottom. By installing the turbine on the dome placed at the top of the draft duct, you can reduce wind velocity leaving the turbine. Thus you can recover more power.

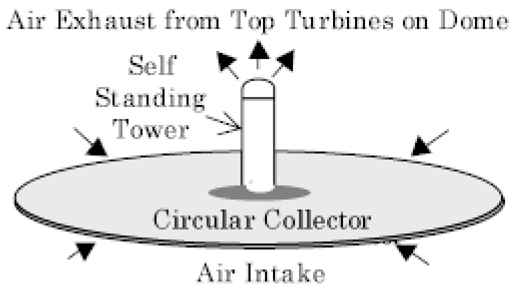

Fig.-4 Tower with Top Turbine

As shown in Fig.-4, installing wind turbine on the dome at the top of the draft duct may increase the construction cost of the draft duct. But a smaller diameter of the draft duct and recovering more power far exceed the increased cost of the top heavy draft duct system.

Number of the turbines are selected from $1+\Sigma 6n$, where n=0, 1, 2, 3, --- And duct diameter is (2n+1) times of that of top turbine. Various type of dome could be considered as shown in Fig. 5. Among them spherical dome would be best as the surface of the dome is 2 times of that of the cross sectional area of the duct. Wind velocity leaving the turbine becomes low enough without interference of surrounding turbines. Spherical dome may require guide vanes for wind turbine fitted near equator.

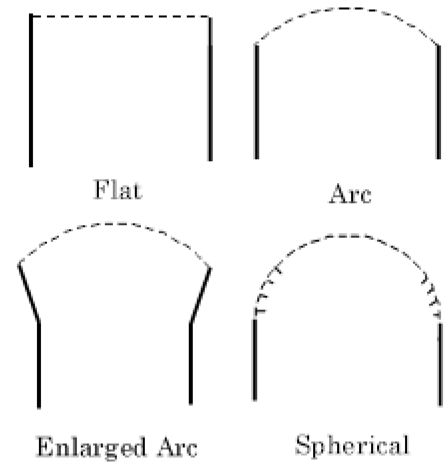

Fig.-5 Dome Type

If you can find a cliff, you can either support the draft duct by the cliff or even drill a vertical shaft and horizontal tunnel through the rock and use the shaft and tunnel for draft duct. In this case, installing wind turbine at the top exit of the draft duct is easier than tower. In this case, you must use semi-circular solar collector as Fig.-6.

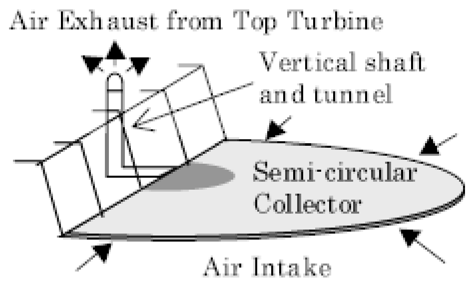

Fig.-6 Vertical Shaft with Semi-circular Collector

For sloped site, rectangular or fan shaped solar collector may be used as illustrated in Fig.-7. Side of the rectangular or fan shaped solar collector is closed to prevent short circuit.

The drawback of the cliff system is an additional friction due to longer duct length and smaller diameter of the shaft. But advantage is that you can use draft height of 2,000 m or even higher.

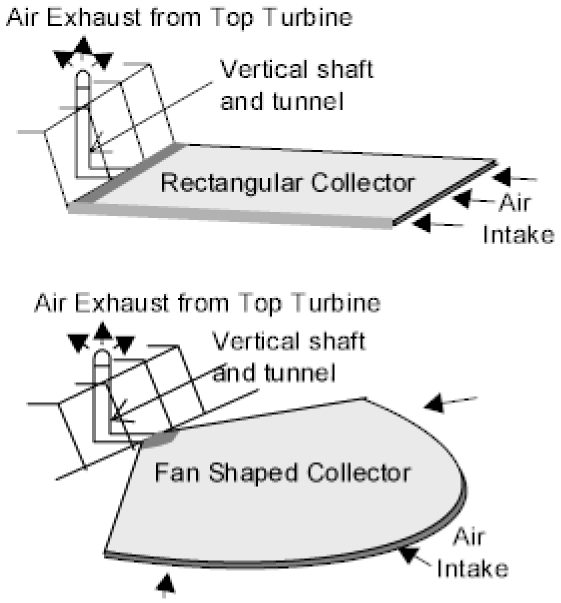

Fig.-7 Rectangular and Fan shaped Collector

Author is going to present the result of several trial designs using the same engineering model consistent with the reverse engineering model of published data. You may find the proposed top turbine concept is far superior to the bottom turbine design. In the course of the study, various alternative ideas were also tested for its effectiveness.

Before going to present the results, let me introduce you the detailed engineering model developed for the sole use of the study.

Solar Collector Model

Solar collector is composed of a flat land covered with either thin plastic film, hard plastic plate and or glass. The cover is supported with many poles and wires. Glass or hard plastic plate will be used as a cover for the place where wind velocity is high.

Most of the solar emission pass through the plastic film and reach earth ground beneath the cover and warm the land surface. Part of the heat is reemitted but the cover recaptures most of them as they are in the infrared spectrum. Heated land warms up air flowing above them.

Detailed heat exchange between sun, cover, earth, air flowing in direct contact with the earth, universe and natural wind blowing above cover is

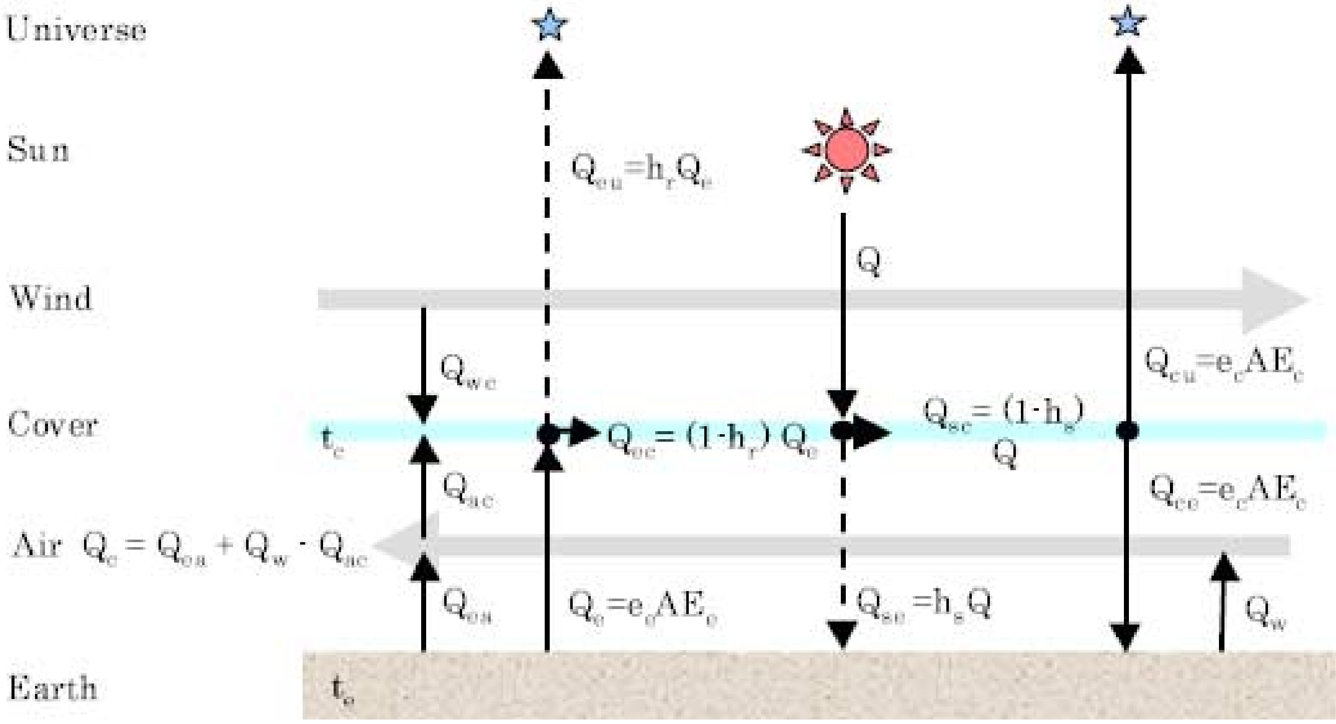

Fig.-8 Solar Collector Model

illustrated in Fig.-8. When you fix temperature rise in the solar collector, you can obtain earth temperature t_e, cover film temperature t_c and heat absorption efficiency of the solar collector η_c (%) by solving heat balance of the solar collector. Detail of the heat balance calculation will be explained in the latter chapter, "Heat Balance Model of Solar Collector".

As the basis of the study, Solar Emission of $1kW/m^2$ was selected according to the standard of IEC60904-1 AM1.5 and the site is just under the sun.

When the diameter of solar collector is d_c (m) and diameter of draft duct is d_t (m), the surface of the solar collector A_c (m^2) is;

$$A_c=(\pi/4)\ (d_c^2 - (1.4d_t)^2)$$

Where, 1.4 is a factor for transition zone from collector to duct.

Total heat energy Q (kcal/h) received by the solar collector becomes;

$$Q=860.1\ A_c$$

Using η_c, you can define heat absorbed by air Q_c (kcal/h) as;

$$Q_c=Q\eta_c/100$$

Q_c (kcal/h) also corresponds mass flows of air and water;

$$Q_c=G(i_i-i_o) + Q_w$$

Here, air flowing into solar collector G (kg/h) is assumed to be dry. Enthalpy of the dry air at temperature of the solar collector inlet t_i °C is i_i (kcal/kgmol) and for temperature at outlet t_o is i_o. Enthalpy of air is calculated by integral form of polynomial analytical expressions of specific heat of Nitrogen and Oxygen.

For Nitrogen;

$$i=6.5(273+t)+0.001/2\ (273+t)^2$$

For Oxygen;

$$i=8,27(273+t)+0.000258/2(273+t)^2+187700/(273+t)$$

Q_w (kcal/h) is heat absorbed by water when water, W (kg/h) is sprayed into solar collector.

$$Q_w = W(t_o-t_i +L_o)$$

Here, specific heat of water is assumed to be 1kcal/kg °C, and latent heat of water at t_o (kcal/kg) is;

$$L_o =598.5-0.595t_o$$

Water content of air in mol. fraction leaving the solar collector is;

$$mf_w= (W/18)\ /((G/28.8)+(W/18))$$

Average molecular weight if wet air is;

$$MW=28.8(1-mf_w) +18mf_w$$

Antoine's Equation calculates vapor pressure of water p_s (mmHg) at t_o;

$$\log_{10} p_s =7.7423 – 1554.16/(t_o+219)$$

Therefore,

$$p_s=10^{(7.7423 – 1554.16/(to+219))}$$

Saturation content of water in air leaving the solar collector, mf_s (-) is;

$$mf_s=13.5951p_s/p_o$$

Therefore, relative humidity of air leaving the solar collector RH (%) is;

$$RH=100\ mf_w/mf_s <100$$

It was assumed that only dry air flows into solar collector. In this case, specific volume of solar collector inlet dry air v_i (m^3/kg) is;

$$v_i=(22.4/28.8)(273+t_i)/(273+0)(10,332/p_i)$$

Where, inlet pressure is p_i (Kg/m^2) and inlet temperature is t_i (°C)

When water is sprayed into solar collector, outlet air contains water. The specific volume of solar collector outlet wet air is v_o (m^3/kg);

$$v_o=(22.4/MW)\ (273+t_o)/(273+0)(10,332/p_o)$$

Where, outlet pressure is p_o (Kg/m^2) and outlet temperature is t_o (°C)

Density of air ρ (kg/m^3) is;

$$\rho=1/v$$

When the height of the cover at air inlet is Z_i and cross sectional area of flow channel of air a_i (m^2), inlet velocity of air u_i (m/sec), becomes;

$$u_i=(G/3,600)\ v_i\ /a_i$$

$$a_i=\pi\ Z_i\ d_c$$

Hydraulic diameter of the air inlet d_{hi} (m) is,

$$d_{hi}=2\ Z_i\ \pi d_c/(Z_i + \pi d_c)$$

Solar collector outlet point is about 1.4 of the draft duct diameter d_t. When the height of the cover at air outlet is Z_o, and $a_o(m^2)$ is cross sectional area of flow channel of air, air outlet velocity u_o(m/sec), is;

$$u_o=((G+W)/3{,}600)\ v_o\ /a_o$$

$$a_o=\pi\ Z_o\ 1.4\ d_t$$

Hydraulic diameter of the air outlet d_{ho} (m) is;

$$d_{ho}=2\ Z_o\ 1.4\pi d_t/(Z_o + 1.4\pi d_t)$$

Hence, average of velocity u (m/sec) and equivalent diameter d_h (m) becomes.

$$u=(u_i+u_o)/2$$

$$d_h=(d_{hi}+d_{ho})/2$$

As Reynolds number $R_e=\rho u d_h/\mu$ is in the transition region of turbulent flow. Friction factor f (-) of the duct wall and air is,

$$1/SQRT(f)=-4\log_{10}((e/d_h)/3.71+1.26/(Re\ SQRT(f)))$$

Here, viscosity of air, μ is 0.018 c.p.=0.000018 kg/m sec and surface roughness of earth e (mm) is 1 mm.

Friction loss of air flowing inside the solar collector, F_h (Kg m/kg) is estimated by applying Fanning equation.

$$F_h= f\ 4\ (u^2/2\ g_c)\ (r_c/d_h)$$

Pressure drop in the solar collector, Δp_h (Kg/m^2) is;

$$\Delta p_h=\rho F_h$$

Solar collector outlet pressure p_o (Kg/m^2) is;

$$p_o=p_i-\Delta p_h$$

Here, $r_c=d_c/2$ is radius of the solar collector and u is average velocity of air, d_h is hydraulic equivalent diameter of the flow channel of air.

Acceleration loss at solar collector inlet F_a (Kg m/kg) and Δp_a (Kg/m^2) are;

$$F_a= (u_i^2/2\ g_c)$$

$$\Delta p_a=\rho F_a$$

Contraction Model

Wind velocity has to be increased by contraction means. When bottom turbines are installed, solar collector outlet velocity is u_1 and turbine inlet velocity is u_2. Even if the bottom turbines are not installed, contraction device is still needed between solar collector and draft duct. In this case, solar collector outlet velocity is u_1, and draft duct inlet velocity is u_2. In the case of duct top turbine, draft duct outlet velocity is u_1 and top turbine inlet velocity is u_2. When no top turbine is installed, top contraction device is not required.

In any case, contraction loss, F_c (Kg m/kg) or Δp_c (Kg/m^2) are;

$$F_c=\alpha\xi u_2^2/2g_c$$

$$\Delta p_c=\rho\ F_c$$

Here, α is a correction factor for smooth contraction. Good agreement with Australian project was obtained when α =0.5.

Coefficient for sudden contraction loss, ξ (-) could be obtained from Rouse data included in Perry's Hand Book as shown in Fig.-9.

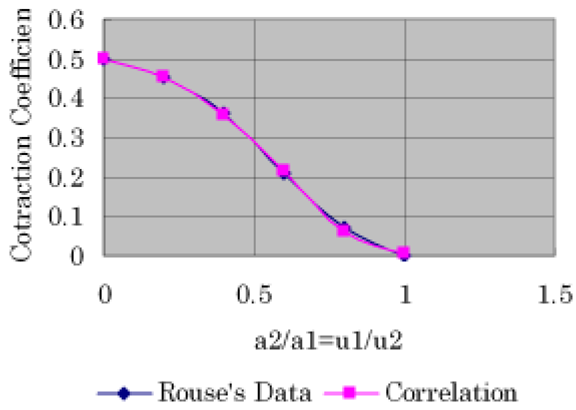

Fig.-9 Coefficient of Sudden Contraction Loss

$$\xi=0.5\ EXP((-10(u_1/u_2)^2+10(u_1/u_2)-5)\ (u_1/u_2)^{2.2})$$

Here,

$$a_2/a_1=u_1/u_2$$

When top turbine is installed, turbine outlet velocity of zero could be applied. Turbine inlet velocity is decided to make draft force to match with total of various losses and recovered power.

Wind Turbine Model

Wind turbine could be either installed at the bottom of the draft duct or at the top of the draft duct. In the case of Australian project, 32 wind turbines are installed around the bottom of draft duct. Numbber of turbines could be 1+Σ6 , where n=0, 1, 2, 3, ---. In this case, duct diameter is (2n+1) times of that of top turbine.

Theoretical power, E (Kgm/sec) recovered by wind turbine installed in a cowling, is described as;

$$E=m\ (u_i^2-u_o^2)/2\ g_c$$

Here, air mass m (kg/sec) is described as;

$$m=(G+W)/3{,}600$$

When turbine blade efficiency is η_b (%), shaft power output (kW) is;

$$\text{Shaft Power}=(\eta_b/100)\ E/101.972$$

When η_g (%) is generator efficiency, generator output (kW) is;

$$\text{Generator Output}=(\eta_g/100)(\text{Shaft Power})$$

Here, η_b=86 % and η_g=098 %.

When u_i (m/sec) is design inlet velocity, and n is number of turbines, r (m) is a blade radius and air specific volume is v_i (m/sec),

$$u_i=(m/n)\ v_i\ /a\ = (m/n)\ v_i/\ (\pi r^2)$$

Hence,

$$r=\mathrm{SQRT}((m/n)\ v_i/(\pi u_i))$$

Outlet velocity of Top Turbine, u_o(m/sec) is;

$$u_o=u_i\ (\text{Area of Turbine}/\text{Area of Dome})$$

Power recovered by turbine F_t (Kg m/kg) and Δp_t (Kg/m^2) are;

$$F_t= (u_i^2-u_o^2)/2\ g_c$$

$$\Delta p_t=\rho\ F_t$$

Draft Duct Model

Ambient temperature t_o (^{o}C) at the top of the draft duct having the height of Z (m) is expressed by following NASA equation.

$$t_o + 273=(t_i + 273) - 0.0065\ Z$$

Barometric pressure at the top of the draft duct p_o (Kg/m^2) is assumed by following equation also published by NASA. Here, p_i is barometric pressure at duct bottom.

$$p_o=p_i\ (1- 0.0065\ Z/(t_0 + 273)5.2569$$

When p_i (Kg/m^2) is inlet pressure and t_i (^{o}C) is inlet temperature, specific volume of the draft duct inlet air v_i (m^3/kg) is calculated by;

$$v_i=(22.4/MW)((273+t_i)/(273+0)(10{,}332/p_i)$$

When p_o (Kg/m^2) is inlet pressure and t_i (^{o}C) is inlet temperature, specific volume of the inlet air to draft duct v_o (m^3/kg) is calculated by;

$$v_o=(22.4/MW)((273+t_o)/(273+0)(10{,}332/p_o)$$

When cross sectional area of the draft duct is a (m^2), duct inlet wind velocity u_i (m/sec) becomes;

$$u_i=((G+W)/3{,}600)\ v_i\ /a$$

Wind velocity at duct outlet u_o (m/sec) becomes;

$$u_o=((G+W)/3{,}600)\ v_o\ /a$$

Average wind velocity u (m/sec) is;

$$u=((G+W)/3{,}600)\ v\ /a$$

Where $v=(v_i+v_o)/2$.

Friction loss of air against draft duct wall F_f (Kg m/kg) and Δp_f (Kg/m^2) are described by Fanning's Equation.

$$F_f=f\ 4\ (u^2/2\ g_c)\ (Z/d_t)$$

$$\Delta p_f=\rho\ F_f$$

As Reynolds number $Re=\rho u d_t/\mu$ of the flow of air in the duct is in turbulent region, friction factor f (-) is calculated by following equation applicable for rough surface in turbulent region.

$$f=(1/(2.28-4\ \log\ (e/d_t)))^2$$

Here, e is rough surface height in mm. As a design basis, 1mm was taken. Air viscosity μ=0.018 c.p.=0.000018 kg/m sec.

When top turbine is not installed, velocity head leaving the system is not recovered and is permanently lost. Those loss, F_e (Kg m/kg) or Δp_e (Kg/m^2) are described by following equation.

$$F_e=u_o^2/2\ g_c$$

$$\Delta p_e=\rho\ F_e$$

Heat Loss Q_t (kcal/h) across draft duct wall is

$$Q_t=A_t\ (k/\zeta)\ (t_i - t_a)$$

When rock wool is used for insulation, thermal conductivity, k = 0.05 (kcal/m/h/^{o}C) For design purpose insulation thickness of ζ=20mm was used.

Surface area of the wall of the duct A_t (m^2) is;

$$A_t = \pi\ d_t\ Z$$

Contraction loss at the bottom of the draft duct F_c and friction loss in the draft duct F_f warms up the air and contribute draft force. Such heat Q_f (kcal/h) is;

$$Q_f=(G+W)\ (F_c + F_f)/J$$

Here, J=423 (Kg m/kcal)

Blade loss of bottom turbine also warms up air. Such heat Q_b (kcal/h) is;

$$Q_b=E\ (1 - \eta_b/100)\ /(G/3{,}600)$$

Temperature drop by isentropic expansion of air Δt (^oC) is estimated by following equation.

$$\Delta t=t_i\ (1-(p_o/p_i)^{((\gamma-1)/\gamma)})$$

Here, γ is isentropic exponent.

$$\gamma = c_p/c_v$$

When R (kcal/kg ^oK) is universal gas constant,

$$c_v = c_p - R$$

Here, R is;

$$R=1.987\ \text{kcal/kg mol}\ ^oK$$

When wet air mol, weight is MW, R (kcal/kg ^oK) is expressed as;

$$R=1.987/MW$$

When wet air is leaving the draft duct at the temperature of t_o (^oC), and pressure of p_o (Kg/m^2), the water saturation vapor pressure, p_s (mmHg) is expressed by following Antoine's equation.

$$\log_{10} p_s = 7.7423 - 1554.16/(t_o + 219)$$

$$p_s=10^{(7.7423\ -\ 1554.16/(to\ +219))}$$

Hence, saturation mol. fraction of water in air, mf_s is;

$$mf_s=13.5951 p_s/p_o$$

Thus, relative humidity of air, RH (%) is expressed as follows.

$$RH=100\ mf_w/mf_s$$

When RH>100%, fog will be formed and latent heat of water condensation may warm up air. Such heat Q_c (kcal/h) is;

$$Q_c = L_o(mf_w-mf_s)(G+W)$$

Here, L_o (kcal/kg) is expressed as;

$$L_o = 598.5-0.595 t_o$$

If temperature of air is below dew point, Q_c(kcal/h) is;

$$Q_c = 0$$

Due to all those heat, draft duct top temperature t_o (^oC) becomes;

$$to=ti - \Delta t + (-Q_t + Q_f + Q_b + Q_c)/((G+W)\ c_p)$$

When average air temperature in the draft duct is $t=(t_i+t_o)/2$ (^oC), specific heat of the dry air C_{pa} (kcal/kgmol^{o}C) is estimated from polynomial analytical expressions of specific heat of Nitrogen and Oxygen.

For Nitrogen;

$$c_{pa}=6.5+0.001\ (273+t)$$

For Oxygen;

$$c_{pa}=8.27+0.000258\ (273+t)-187{,}700/(273+t)2$$

Specific heat of steam c_{pw} (kcal/kgmol ^oC) is;

$$c_{pw}= 8.22+0.00015\ (273+t)+0.00000134(273+t)2$$

Hence, specific heat of wet air c_p (kcal/kg^{o}C) becomes;

$$c_p=(c_{pa}(1-mf_w)+c_{pw} mf_w)/MW$$

Here, MW is average molecular weight of wet air and mf_w is mol. fraction of water.

Top temperature of the draft duct t_o (^oC) is determined by the combination of the following factors;

Temperature drop by wall heat loss $=Q_t/((G+W)c_p)$

Temperature rise by bottom contraction and friction loss $=Q_f/((G+W)c_p)$

Temperature rise by bottom turbine blade loss $=Q_b/((G+W)c_p)$

Temperature rise by water condensation $=Q_c/((G+W)c_p)$

Draft Force Balance

Driving force of draft effect of the duct, Δp_{dl} (Kg/m^2) is expressed as;

$$\Delta p_{dl}=(\rho_o - \rho_i)\ Z$$

Here, ρ_o is average air density outside duct and ρ_i

is average air density inside duct.

The sum of acceleration loss, friction loss, contraction loss, recovered power, and unrecovered velocity head (Kg/m^2) is;

$$\Delta p_l=\Delta p_a + \Delta p_h + \Delta p_c + \Delta p_f + \Delta p_t + \Delta p_e$$

Here, Δp_a is acceleration loss, Δp_h is collector friction loss, Δp_c is contraction loss, Δp_f is friction loss of duct, Δp_t is recovered power by turbine, Δp_e is unrecovered velocity head leaving the system.

The system operates at equilibrium point.

$$\Delta p_{dl}= \Delta p_l$$

Heat Balance Model of Solar Collector

As already explained in "Solar Collector Model", You can obtain temperature of the earth t_e, temperature of the cover film t_c and heat absorption efficiency of the solar collector η_c (%) by solving heat balance of the solar collector.

Detailed heat exchange between sun, cover film, earth, air flowing in direct contact with earth, universe and natural wind blowing above plastic cover is illustrated in Fig-6.

Infrared fraction of the solar emission Q (kcal/h) will be absorbed by cover as described below;

$$Q_{sc}=a_s Q \quad \text{(kcal/h)}$$

Where a_s (dimensionless) is absorptivity of solar emission by cover.

Non infrared fraction of the solar emission Q_{se} will pass through the cover and reach earth surface.

$$Q_{se}= Q - Q_{sc} = Q\ (1-a_s) \quad \text{(kcal/h)}$$

Here, (1- a_s) is defined as transparency of the cover as regard for solar emission, η_s=(1- a_s), then Solar emission absorbed by collector cover Q_{sc}(kcal/h) becomes;

$$Q_{sc}=Q\ (1-\eta_s)$$

Solar emission Q_{sc} (kcal/h) reached at the surface of the earth becomes;

$$Q_{se}= Q\ \eta_s$$

For design purposes, η_s=0.6 was used.

When temperature of the cover is t_c, the black body emission of the cover E_c (kcal/m^2h) is expressed by Stefan-Botzmann's equation

$$E_c=4.88((t_c+273)/100)^4$$

When emissivity of the collector cover is ε_c (dimensionless), heat loss from the cover to universe Q_{cu} (kcal/h), and heat loss from the cover to earth Q_{ce} becomes;

$$Q_{cu}=Q_{ce}=A_c\ \varepsilon_c\ E_c$$

For design purpose ε_c=0.85 was used.

When temperature of the earth surface is t_e (°C), the emission of the earth E_e(kcal/m^2h) is expressed by Stefan-Botzmann's equation.

$$E_e=4.88\ ((t_e+273)/100)^4$$

When emissivity of the earth surface is $\varepsilon_e = a_e$, the heat loss from the earth Q_e (kcal/h) becomes;

$$Q_e=A_c\ \varepsilon_e\ E_e$$

For design purpose, emissivity of the earth $\varepsilon_e = 0.4$ was taken.

Cover as Q_{ec} (kcal/h) again absorbs some portion of the infrared radiation from the earth;

$$Q_{ec}=Q_e\ a_c$$

Here, a_c is absorptivity of the cover.

The rest of the heat Q_{eu} (kcal/h) is permanently lost to the universe.

$$Q_{eu}= Q_e\ (1-a_c)$$

When, η_c is defined as transparency of the cover with respect to infrared ray, $\eta_c = (1-a_c)$, then

$$Q_{ec}=Q_e\ (1-\eta_c)$$

$$Q_{eu}= Q_e\ \eta_c$$

For design purpose, transparency of the cover η_c = 0.05 was taken.

Forced convection heat transfer coefficient between air and earth or cover, h_f (kcal/m^2h°C) is calculated by Nusselt type equation as flow is in turbulent zone.

$$h_f=0.036R_e^{0.8}\ P_r^{(1/3)}\ (k/r_c)$$

Where $R_e=\rho\ ur_c/\mu$ is Reynolds number, $P_r=c_p\mu 3{,}600/k$ is Prandtle number, k=0.0276(kcal/mh°C) is thermal conductivity of air

and r_c(m) is diameter of the collector.
Natural convection heat transfer coefficient between air and flat earth, h_n (kcal/m^2 h °C) is;

$$h_n=1.3\ \Delta t^{1/3}$$

Using this coefficient, heat transfer between earth surface and air Q_{ea} (kcal/h) could be;

$$Q_{ea}=A_c\ (h_f + h_n)\ LMTD_{ea}$$

Where, $LMTD_{ea}$ is mean logarithmic mean temperature difference between earth and air.

$$LMTD_{ea}=(\ \Delta t_i\text{-}\ \Delta t_o)/(2.3\log(\Delta t_i/\Delta t_o))$$

Here $\Delta ti=t_e\text{-}t_i$ is temperature difference at inlet and $\Delta t_o=t_e\text{-}t_o$ is temperature difference at outlet.
Similarly, heat transfer between cover and air Q_{ac} (kcal/h) could be expressed as;

$$Q_{ac}=A_c\ h_f\ LMTD_{ac}$$

In the same analogy, heat transfer between cover and natural wind Q_{wc} (kcal/h) could be;

$$Q_{wc}=A_c\ h_w\ LMTD_{wc}$$

Film coefficient of natural wind h_w is a function of natural wind velocity u_w. For design purpose u_w=10 m/sec was taken.
Heat balance around solar collector cover becomes

$$Q_{sc} + Q_{ec}+ Q_{ac} + Q_{wc}= Q_{cu} + Q_{ce}$$

Water prayed into the collector will have direct contact with earth surface having the temperature of t_e (°C) and evaporate instantly. The water take heat of Q_w (kcal/h).

$$Q_w = W(t_e\text{-}t_i + L_e)$$

Where, latent heat of water L_e (kcal/kg) is;

$$L_e = 598.5\text{-}0.595t_e$$

And water specific heat is 1kcal/kg°C.
Heat balance around earth becomes.

$$Q_{se} + Q_{ce}= Q_{ea} + Q_e + Q_w$$

Hence, heat absorption efficiency of the solar collector, η_c (%) is;

$$\eta_c=100Q_c/Q =100\ (Q_{ea} + Q_w\text{-}\ Q_{ac})/Q$$

Water Supply System

This model was added to find out effectiveness of water injection into the solar collector.
Power consumption of pump supplying water to the solar collector (kW) is;

$$PowerConsumption=0.0098067(W/3,600)\ h(\eta_p/100)$$

Here, W (kg/h) is pump capacity, h (m) is pump head and η_p is pump efficiency. For design purpose h=100 m, and η_p =70 % was taken.

Concrete Volume of Self-standing Tower

Seismic factor is no longer controlling structural design of tall tower when the height of the tower is more than 500m. Wind force determines the required concrete volume. Following design criteria were assumed.
Design wind velocity u_b at tower bottom;

$$u_b=80\ \text{m/sec}$$

Design wind velocity u_t at tower top;

$$u_t=120\ \text{m/sec}$$

Design strain of reinforced concrete;

$$\sigma=12{,}000\text{kN/m}^2$$

Design density of reinforced concrete;

$$\rho_{\ RC}=24\text{kN/m}^3$$

Top turbine and dome system weight per cross sectional area of the duct=100kg/m^2

For quick estimation, tower was split into 3 sections.

Top section; from top to 50% from the top
Middle section; 50% to 80% from the top
Bottom section; 80% to 100% from the top

For each section, required wall thickness was estimated from combined strain caused by bending moment and its own dead weight.
Design wind lord w (kN/m) at tower top and bottom;

$$w=d_t\rho u^2/2000$$

Where, ρ is air density of the wind and d_t is tower diameter.
Bending moment M_b (kN-m) at tower bottom;

$$M_b=(2w_t+w_b)/6*l2$$

Bending moment M_x (kN-m) at x (m) from the top;

$$M_x=-w_tx^2/2\text{-}(w_b\text{-}w_t)x^3/(6Z)$$

Bending Strain σ (kN/m^2) is;

$$\sigma = M/C$$

Here, cross sectional factor C (m^3) for each section is ;

$$C = \pi/(32d_o)(d_o^4 - d_i^4)$$

Concrete volume V (m^3) for each section is;

$$V = (1/3)\pi h(R_o^2 + R_o r_o + r_o^2) - \pi r_i^2$$

Where, h is height of each section, R_o is bottom outside radius, r_o is top outside radius and r_i is inside radius.

Construction Cost

For comparison of various different designs, uniform universal construction cost was applied as follows;

Composite unit cost of the solar collector per collector surface (yen/m^2);

$$1{,}000 + 20(Z_i + Z_o)$$

Here, Z_i is collector inlet height, Z_o is collector outlet height.

Composite unit cost of wind turbine system per power output;

30,000 (yen/kW)

Composite unit cost of water system per power consumption;

50,000 (yen/kW)

Two types of draft duct were compared.

(1) Self-standing Tower

Composite unit cost of tower and foundation per volume of reinforced concrete (RC) of the tower;

15,000 (yen/m^3)

(2) Shaft and tunnel drilled through the cliff rock

Drilling cost per excavation volume;

3,000 (yen/m^3)

$$\text{Volume of excavation} = (\pi/4)d_t^2 L$$

$$L = Z(1 + 1/\tan(\pi\theta/180))$$

Here, θ (degree) is inclination of the cliff, L (m) is a total length of the vertical shaft and horizontal tunnel.

For design purpose, θ =70 degree. was selected.

Results of the Trial Design of Different Concepts

As shown in Case-A Table-2, the calculated results of the model meet published data of Australian Project very well. Power output is 202 MW and thermal efficiency of the power generation system is 1.03%. Total initial investment is 62,769 million yen (738million Australian $) Thus, unit cost of power generation becomes 20.9 yen/kWh (19 cents/kWh).

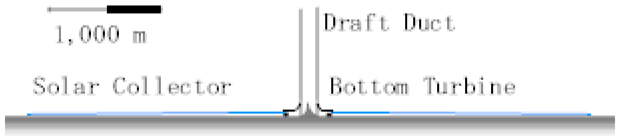

Fig.-10 Cross Sectional View of Case-A

Case-B is optimization of bottom turbine concept. Wind turbines are placed at the bottom of the tower as Case-A. Diameter of solar collector of 5 km remained also the same as Case-A. But temperature rise in collector and tower height was optimized. Temperature rise of 3 °C and tower height of 1,200 m showed best performance. Tower diameter of 800 m and height of 1,200 m requires reinforced concrete of 6.05 million-m^3. Initial investment is tripled up to 185,406 million-yen. But power recovery is enhanced up to 668MW and thermal efficiency of the power generation system is also increased up to 3.58%. As the results, unit cost of power generation was reduced down to 18.6 yen/kWh.

Case-C adopted top turbine concept. Wind turbines are placed on top of the draft tower. Tower heights of 1,000 m, diameter of solar collector of 5 km and temperature rise in collector of 35°C were taken as same as Case-A. Only difference is smaller diameter of the tower of 110 m against of 150 m of Case-A. Power recovery was increased up to 273 MW and thermal efficiency of the power generation system is 1.21%. On the contrary to smaller diameter of tower, concrete volume of 1.4 million-m^3 remained almost same as

Case-A due to thick wall. Initial investment is 68,375 million-yen. Thus, unit cost of power generation became 19.0 yen/kWh.

Case-D is optimization of Case-C. Wind turbines are also placed on top of the tower. Diameter of solar collector is 5 km. But temperature rise in collector and tower height was optimized. Temperature rise of 3 °C and tower height of 1,200 m showed best performance. Tower diameter of 535 m and height of 1,200 m requires reinforced concrete of 4.84 million-m^3. Initial investment is 178,328 million-yen. But power recovery is greatly enhanced up to 826 MW and thermal efficiency of the power generation system is 4.3% which is the heighest of all case. As the results, unit cost of power generation was reduced down to 14.1 yen/kWh.

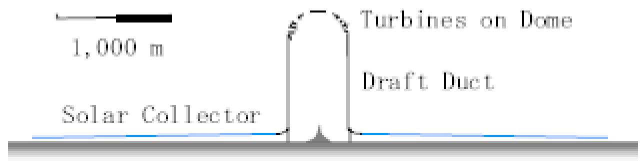

Fig.-11 Cross Sectional View of Case-D

Case-E is the case to use shaft and tunnel in the cliff side rock as draft duct. Wind turbines are placed on top of the draft duct i.e. cliff top. Shaft and tunnel are drilled through the rock along the cliff having the inclination of 70 degree. Temperature rise of 35 °C and height of the vertical shaft was taken 1,000 m. Semi-circular solar collector having the diameter of 5 km was selected for the study. The diameter of the vertical shaft and tunnel became 82 m. Power recovery of 115 MW and thermal efficiency of the power generation system is 0.58% were achieved. Initial investment is 50,015 million-yen. Unit cost of power generation became 29.0 yen/kWh.

Case-F is optimization of Case-D. Wind turbines are also placed on top of the draft duct. As excavation cost prohibit selecting low temperature rise. Therefore, temperature rise of 35 °C and height of the shaft was taken 2,000 m. Semi-circular solar collector having the diameter of 5 km was selected for the study. The diameter of the vertical shaft and tunnel became 67 m. Power recovery of 263 MW and thermal efficiency of the power generation system is 1.34% were achieved. Initial investment is 63,467 million- yen. Unit cost of power generation became 15.9 yen/kWh.

Conclusions

After reviewing the results, we can see the big advantage of top turbine concept.

Combination of top and bottom turbine found no advantage over top turbine configuration.

Hybrid of this system with solar cell was also tested but no advantage was found.

Effectiveness of installing hot plate in the air above the earth was also tested and found no advantage over simple earth.

Water injection into solar collector showed no advantage, as the water consumes lot of solar heat in latent heat of evaporation and heat remained for air heating is greatly reduced.

Final selection of the temperature rise in solar collector, height of draft duct and type of construction of the draft duct i.e. tower or combination of shaft and tunnel is will be done after careful study of construction cost for each specific site. In the same way, type of solar collector could be finalized between semi-circular and rectangular type.

Optimization of Top Turbine Concept

As shown from Fig.-12 to 19, optimization of height of the draft duct and temperature rise in the collector was conducted for the combination of circular collector and self-standing draft tower. In this study, self standing concrete tower was selected and diameter of the solar collector was fixed at 5 km. Draft height of 1,000, 1,200, 1,400 m had been selected. For each draft height, a set of temperature rise in the collector of 3, 5, 10, 20, and 35 °C were selected respectively.

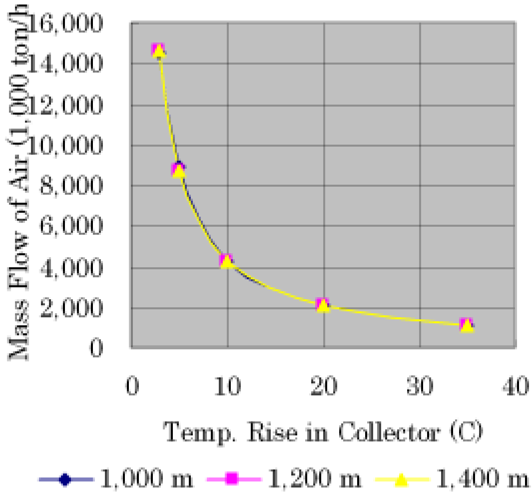

Fig.-12 Mass Flow of Air

As shown in Fig.-12, small temperature rise in solar collector results in larger mass flow of air. When the amount of solar emission received by the solar collector is fixed, a mass flow of air is proportional to inverse of temperature rise in the solar collector. Tower height has no impact on mass flow of air.

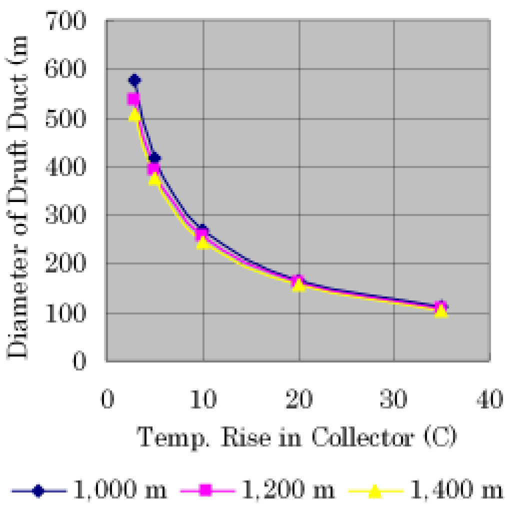

Fig.-13 Diameter of Duct

Naturally, diameter of the draft duct also increases along with mass flow of air as shown in Fig.-13. Tower height has small impact on tower diameter.

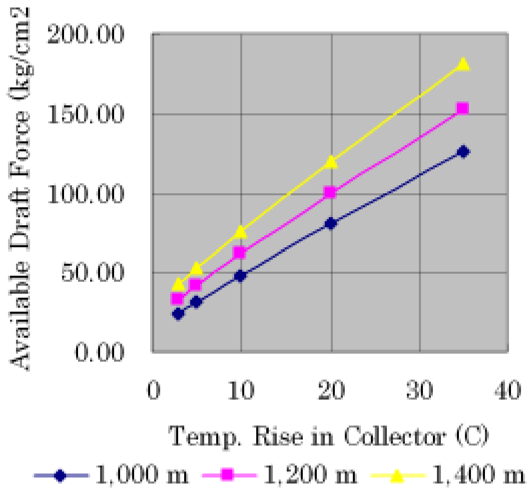

Fig.-14 Available Draft Force

As shown in Fig.-14, available draft force is almost proportional to temperature. Increase of draft height also increase draft force.

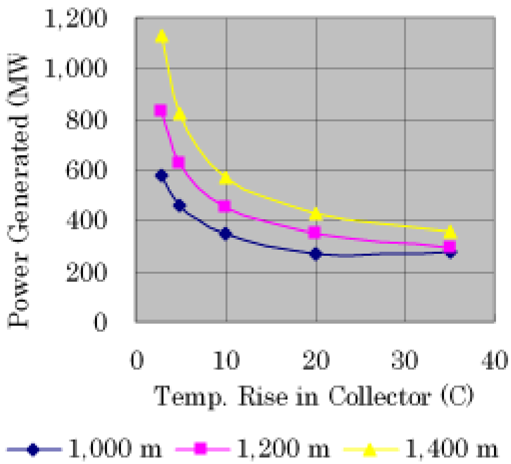

Fig.-15 Power Generated

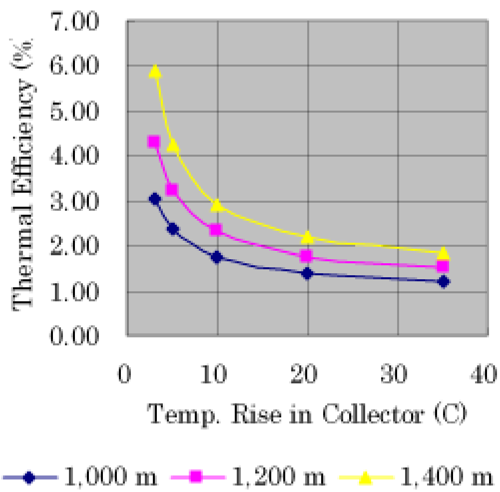

Fig.-16 Thermal Efficiency

As shown in Fig.-15, power generated greatly increases at lower temperature rise due to mainly increased mass flow rate of air.

As shown in Fig.-16, thermal efficiency of the power generation system is proportional to power generated.

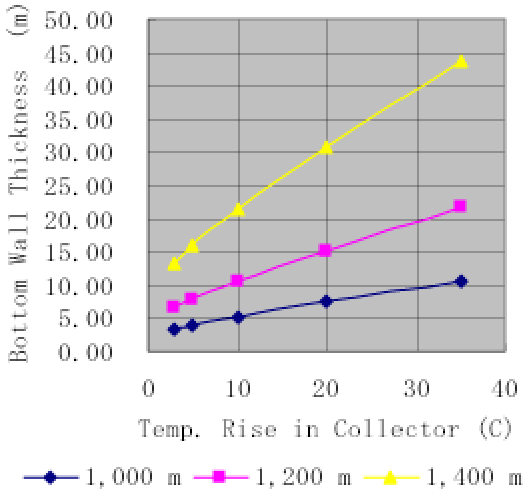

Fig.-17 Wall Thickness at Tower Bottom

As shown in Fig.-17, wall thickness increase when tower became slender in higher temperature rise design.

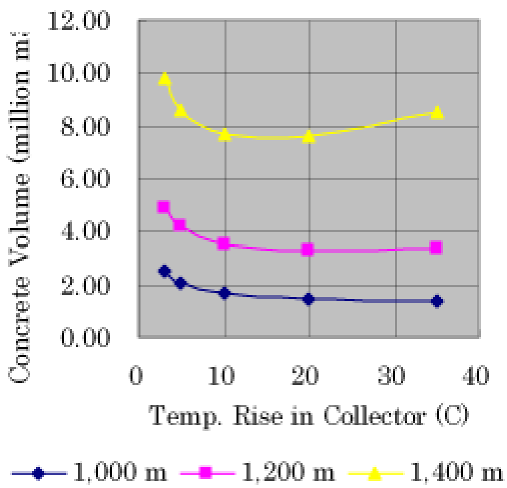

Fig.-18 Concrete Volume

As shown in Fig.-18, small temperature rise increases concrete volume by increased diameter. But big temperature rise also increases concrete volume by increased wall thickness. Minimum concrete volume of tower having the height of 1,400m is achieved at temperature rise of 10 °C. In the same way, minimum concrete volume of tower having the height of 1,200m is achieved at temperature rise of 20 °C. Minimum concrete volume of tower having the height of 1,000m is achieved at temperature rise of 35 °C. This might be the reason of why Australian project used temperature rise of 35 °C.

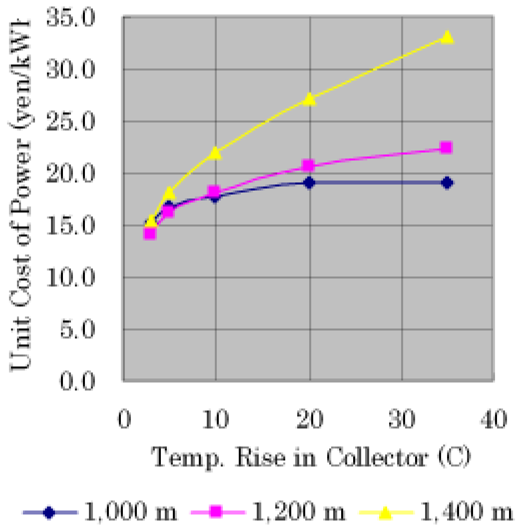

Fig.-19 Unit Cost of Power Generation

As shown in Fig.-19, the lowest unit cost of power generation was achieved when draft height is 1,200m and temperature rise is 3 °C. As the design of the tower does not consider buckling, optimum design preferred small temperature rise.

This problem may be solved later by introducing such failure into design model. In any case, optimum design should be finalized based on accurate construction cost.

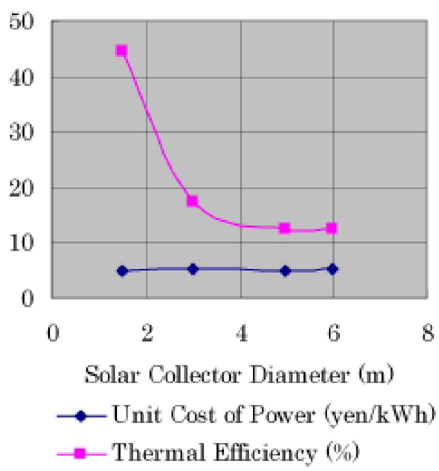

Fig.-20 Unit Cost v.s. Collector Diameter

As previous study were conducted keeping the diameter of the solar collector at 5 km, optimization of the size of the collector were conducted fixing the duct height at 1,200 m and temperature rise at 3 °C.

As shown in Fig.-20 it was found that solar collector diameter of 5 km is the optimum size.

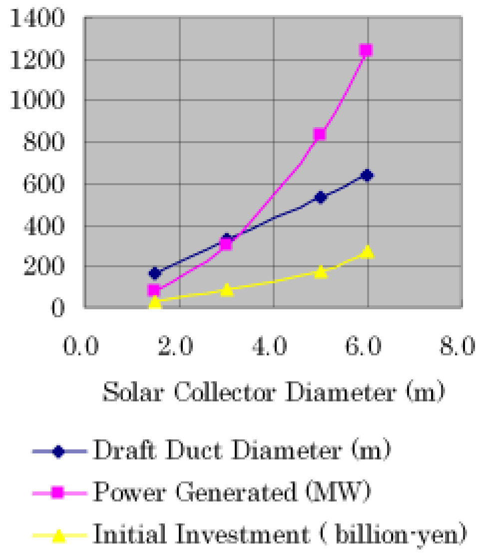

Fig.-21 Duct Diameter v.s. Collector Diameter

Other related data are shown in Fig.-21.

Detail data such as initial investment, number of top turbines, diameter of top turbine, velocity at top turbine inlet, heat recover efficiency of the collector, temperature drop by isentropic expansion were summarized in Table-3.

Final Word

Japan's annual power consumption in 1997 was 1 trillion kWh. If we install wind turbines along the coast of Japan with width of 3 km, annual power generation reaches 28 % of total consumption. Japanese Island is covered with forest of 66 %. If you are allowed to use this forest as a sustainable energy source, you can supply 12 % of total consumption. Rest of the 60 % could be easily supplied by solar cell.

In other words, Japan could be independent on energy supply even when earth derived energy is depleted.

I believe the "Power Generation by Artificial Typhoon" can help to supplement windfirm scheme.

Acknowledgement

Author has special acknowledgement for Dr. H. Morinaga and for Dr. D. T. Chiba.

Table-2 Summary of the Results

Case		A	B	C	D	E	F
Design Concept		Austral	Opt. Bottom	Top	Opt. Top	Shaft Top	Opt. Shaft Top
Type of Solar Collector		Circular	Circular	Circular	Circular	Semi-Circular	Semi-Circular
Type of Draft Duct	Unit	Tower	Tower	Tower	Tower	Shaft	Shaft
Diameter of Solar Collector	m	5,000	5,000	5,000	5,000	5,000	5,000
Height of Collector Cover at Inlet	m	10	50	10	50	10	10
Height of Collector Cover at Outlet	m	30	100	40	100	75	70
Height of Draft Duct	m	1,000	1,200	1,000	1,200	1,000	2,000
Diameter of Draft Duct	m	150	800	110	535	82	67
Wall Thickness of Duct at Bottom	m	8.09	5.38	10.63	6.6	NA	NA
Concrete Volume	million-m^3	1.43	6.05	1.4	4.84	NA	NA
Number of Bottom Turbine	-	32	32	0	0	0	0
Diameter of Bottom Turbine	m	16.3	78.7	NA	NA	NA	NA
Number of Top Turbine	-	0	0	37	169	19	19
Diameter of Top Turbine	m	NA	NA	15.4	35.5	15.3	13.1
Barometric Press. at Collector Inlet	kg/m^2	10,332	10,332	10,332	10,332	10,332	10,332
Barometric Press. at Duct Outlet	kg/m^2	9,219	9,008	9,219	9,008	9,219	8,205
Temp. Rise in Solar Collector	°C	35	3	35	3	35	35
Ambient Temp. at Draft Duct Outlet	°C	23.50	22.20	23.50	22.20	23.50	17.00
Temp. of Solar Collector Cover	°C	33.50	27.70	33.50	27.10	33.60	33.50
Temp. of Collector Earth	°C	97.30	83.30	97.00	77.80	100.40	97.80
Temp. of Air at Draft Duct Outlet	°C	63.03	31.75	62.87	31.69	62.81	60.92
Temp. Drop by Adiabatic Expansion	°C	2.12	1.31	2.11	1.31	2.12	4.22
Temp. Drop by Wall Heat Loss	°C	0.16	0.01	0.12	0.00	0.23	0.40
Temp. Rise by Contraction and Friction	°C	0.19	0.04	0.12	0.00	0.16	0.54
Temp. Rise by Bottom Turbine Loss	°C	0.11	0.03	0.00	0.00	0.00	0.00
Heat Absorption Efficiency of Collector	%	52.34	60.69	52.34	61.67	52.2	52.32
Mass Flow Rate of Air	1,000 ton/h	1,074	13,941	1,075	14,580	537	538
Velocity at Solar Collector Inlet	m/sec	1.64	4.26	1.64	4.45	1.64	1.64
Velocity at Solar Collector Outlet	m/sec	14.53	9.60	14.87	15.01	11.16	13.95
Velocity at Bottom Turbine Inlet	m/sec	43.22	21.32	NA	NA	NA	NA
Velocity at Draft Duct Inlet	m/sec	16.27	6.72	30.28	15.71	30.04	40.82
Velocity at Draft Duct Outlet	m/sec	18.12	7.67	33.71	17.94	33.44	50.76
Velocity at Top Turbine Inlet	m/sec	NA	NA	46.58	23.76	45.90	69.45
Velocity of Air leaving the System	m/sec	18.12	7.67	16.85	8.97	16.72	25.38
Available Draft Force	kg/m^2	125.48	32.94	125.23	32.80	125.16	272.70
Acceleration Loss at Collector Inlet	kg/m^2	0.16	1.07	0.16	1.17	0.16	0.16
Friction Loss of Solar Collector	kg/m^2	4.93	0.59	5.14	1.14	3.09	4.58
Contraction Loss at Bottom	kg/m^2	19.24	4.50	7.19	0.06	8.83	17.01
Recovered Power by Bottom Turbine	kg/m^2	84.81	23.94	0.00	0.00	0.00	0.00
Friction Loss of Duct	kg/m^2	0.75	0.03	3.70	0.22	7.39	34.57
Contraction Loss at Top	kg/m^2	0.00	0.00	5.91	1.32	5.55	11.20
Recovered Power by Top Turbine	kg/m^2	0.00	0.00	89.62	24.78	86.86	177.80
Unrecovered velocity head	kg/m^2	15.60	3.01	13.50	4.12	13.29	27.41
Power Generated	MW	202	668	273	826	115	263
Thermal Efficiency of Power Generation	%	1.03	3.58	1.21	4.30	0.58	1.34
Annual Power Generation	TWh	322	1,068	379	1,320	183	420
Cost of Solar Collector	million-yen	35,281	74,599	39,233	76,777	26,495	25,516
Cost of Draft Duct	million-yen	21,441	90,769	20,952	72,656	19,553	28,853
Cost of Turbine Generator System	million-yen	6,047	20,033	8,191	28,895	3,968	9,106
Initial Investment	million-yen	62,769	185,406	68,375	178328	50,015	63,467
Unit Cost of Power Generated	yen/kWh	**20.9**	**18.6**	**19.0**	**14.1**	**29.0**	**15.9**

Table-3 Optimization of Top Turbine Concept

Temperature Rise in Solar Collector (°C)	3	5	10	20	35
Mass Flow of Air (1,000 ton/h))					
1,000 m	14,491	8,863	4,259	2,029	1,075
1,200 m	14,580	8,697	4,268	2,032	1,076
1,400 m	14,648	8,723	4,276	2,033	1,076
Diameter of Draft Duct (m)					
1,000 m	575	417	267	166	110
1,200 m	535	393	254	159	106
1,400 m	505	373	243	155	103
Available Draft Force (kg/cm^2)					
1,000 m	24.08	31.02	47.96	80.28	125.23
1,200 m	32.80	40.99	61.01	99.25	152.39
1,400 m	43.11	52.52	75.56	119.47	180.58
Power Generated (MW)					
1,000 m	578	461	344	272	273
1,200 m	826	627	449	345	295
1,400 m	1,129	824	571	430	358
Thermal Efficiency of Power Generation (%)					
1,000 m	3.02	2.38	1.76	1.39	1.21
1,200 m	4.30	3.23	2.30	1.76	1.50
1,400 m	5.87	4.24	2.92	2.19	1.82
Wall Thickness of Duct at Bottom (m)					
1,000 m	3.36	3.96	5.23	7.46	10.63
1,200 m	6.60	7.82	10.41	15.05	21.63
1,400 m	13.33	15.87	21.28	30.65	43.54
Concrete Volume (million-m^3)					
1,000 m	2.51	2.08	1.69	1.46	1.40
1,200 m	4.84	4.14	3.52	3.24	3.35
1,400 m	9.79	8.61	7.67	7.62	8.48
Initial Investment (million-yen)					
1,000 m	134,390	116,999	91,947	78,344	68,375
1,200 m	178,328	158,839	123,093	107,571	99,569
1,400 m	263,234	227,697	189,617	176,026	178,659
Unit Cost of Power Generated (yen/kWh)					
1,000 m	15.2	16.7	17.6	19.0	19.0
1,200 m	14.1	16.1	18.0	20.5	22.3
1,400 m	15.3	18.1	21.9	27.1	33.1
Number and Diameter (m) of Top Turbine					
1,000 m	169 x 38.5	127 x 31.1	91 x 24.1	61 x 18.2	37 x 15.4
1,200 m	169 x 35.8	127 x 30.1	91 x 22.9	61 x 17.4	37 x 14.7
1,400 m	169 x 33.6	127 x 28.5	91 x 21.8	61 x 16.7	37 x 14.2
Velocity at Top Turbine Inlet (m/sec)					
1,000 m	19.94	23.00	28.28	36.37	46.58
1,200 m	23.76	26.75	32.27	40.93	51.86
1,400 m	27.67	30.60	36.31	45.43	56.98
Velocity at Top Turbine Inlet (m/sec)					
1,000 m	7.55	8.63	10.51	13.36	16.85
1,200 m	8.97	9.98	11.91	14.90	18.56
1,400 m	10.34	11.36	13.33	16.05	20.09
Heat Absorption Efficiency of Collector (%)					
1,000 m	61.51	60.56	59.14	56.30	52.34
1,200 m	61.67	60.70	59.24	56.36	52.35
1,400 m	61.80	60.81	59.32	56.39	52.35
Temp. Drop by Isentropic Expansion (°C)					
1,000 m	1.09	1.16	1.32	1.64	2.12
1,200 m	1.31	1.39	1.58	1.97	2.54
1,400 m	1.53	1.62	1.85	2.29	2.96